Proc. Natl. Acad. Sci. USA
Vol. 95, pp. 4870–4875, April 1998
Biochemistry

Experimental support for a β-propeller domain in integrin α-subunits and a calcium binding site on its lower surface

CLAUS OXVIG AND TIMOTHY A. SPRINGER*

Department of Pathology, The Center for Blood Research and Harvard Medical School, 200 Longwood Avenue, Boston, MA 02115

Contributed by Timothy A. Springer, February 23, 1998

ABSTRACT **Integrins are large, heterodimeric surface molecules of wide importance in cell adhesion. The N-terminal half of all integrin α-subunits contains seven weak sequence repeats of ≈60 amino acids that are important in ligand binding and have been predicted to fold cooperatively into a single β-propeller domain with seven β-sheets. We provide evidence supporting this model with a mouse mAb to human Mac-1 (αMβ2, CD11b/CD18). This antibody, CBRM1/20, binds to amino acid residues that are in different repeats and are 94 residues apart in the primary structure in the loop between strands 1 and 2 of β-sheet 5 and in the loop between strands 3 and 4 of β-sheet 6. The 1–2 loops of β-sheets 5–7 in integrins have EF hand-like Ca^{2+}-binding motifs. CBRM1/20 binds to Mac-1 in the presence of Ca^{2+} or Sr^{2+} with an EC_{50} of 0.2 mM. Mg^{2+} or Mn^{2+} cannot substitute. Antibodies to other epitopes on the Mac-1 β-propeller domain bind in the absence of calcium. mAb CBRM1/20 does not block ligand binding. Thus, the region on the lower surface of the β-propeller domain to which mAb CBRM1/20 binds does not bind ligand and, furthermore, cannot bind other integrin domains, such as those of the β-subunit.**

Found on almost all cells of multicellular organisms, integrins play a pivotal role in cellular adhesion. They are large, heterodimeric surface receptors generally comprised of an α-subunit of ≈1,000 and a β-subunit of ≈800 amino acids (1, 2). The N-terminal half of the α-chain consists of seven repeats with weak homology to one another denoted Phe-Gly, Gly-Ala-Pro (FG-GAP) repeats (3); the three or four most C-terminal repeats contain a putative cation binding motif (4). The repeats are interrupted in some integrins by insertion of a domain of ≈200 residues called the "I" domain.

Several regions within the integrin α- and β-subunits, mainly in their N-terminal halves, have been implicated in ligand binding. As a rule, ligand binding to integrins depends on the presence of divalent cations (5). I domains, when present, have been demonstrated to play an important role in ligand binding (6–8). Integrin-mediated adhesion is regulated tightly by complex and little-understood mechanisms that involve both the intra- and extracellular domains (2, 9–12).

Structural knowledge on integrins is limited. Isolated I domains have been expressed in bacteria, and their crystal structures have been solved (13, 14). No atomic level insight has been obtained for other domains. However, it has been predicted that the seven N-terminal FG-GAP repeats fold into a β-propeller, a toroidal all β-structure (3). Previously, the repeats were thought of as independently folded domains, but in this model, they fold into a single, compact domain. Seven β-sheets, each called a W and containing four antiparallel β-strands, are ordered around a pseudosymmetry axis like blades in a propeller (15) (Fig. 1). β-propellers are known from several proteins, including the β-subunit of the heterotrimeric G protein transducin (16) and galactose oxidase (17).

Putative Ca^{2+} binding motifs are present in integrins that are similar to those in EF hands (4). Ca^{2+} has been reported to bind to integrins, including αIIbβ3 (18, 19), but whether the binding sites correspond to the cation-binding motifs is not known. Removal of Ca^{2+} from αIIbβ3 can induce subunit dissociation and inhibit ligand binding (18). On the other hand, the combined absence of Ca^{2+} and presence of Mg^{2+} can stimulate ligand binding by other integrins (20, 21). The β-propeller model predicts that the Ca^{2+} binding motifs are close to one another (on the lower surface of the β-propeller in the loops connecting β-strands 1 and 2) in W5, W6, and W7 (Fig. 1). A possible direct role in ligand binding for the Ca^{2+} bound to these motifs has been proposed often. The effect of Ca^{2+} on the conformation of the β-propeller domain is unknown.

To test the β-propeller fold, we sought a mAb to an epitope that would contain residues that were distant in the amino acid sequence and thus would place constraints on the fold. Here, we describe such a mAb to Mac-1 (αMβ2, CD11b/CD18), an integrin on leukocytes that binds ligands including intercellular adhesion molecule-1, iC3b, and fibrinogen (22). The mAb recognizes residues in the 1–2 loop of W5 containing a Ca^{2+}-binding motif and the 3–4 loop of W6 of the Mac-1 α-subunit. Of interest, the mAb requires Ca^{2+} for binding to Mac-1. Furthermore, its footprint is predicted to include a substantial portion of the bottom of the β-propeller domain, yet it does not block ligand binding by Mac-1 or affect α- and β-subunit association.

MATERIALS AND METHODS

DNA Constructs and Mutagenesis. The majority of the coding sequence of the human αM subunit cDNA, nucleotides 73–3534 (23), was excised by full and partial digestion with *Xba*I and *Xma*I, respectively, and was cloned into the *Xba*I site of pCDNA3.1+ (Invitrogen) by using a linker that reconstructed the remaining 14 coding nucleotides and provided a stop codon and a *Xba*I site. PCR primers were synthesized that allowed ligation into the *Not*I/*Sac*I sites of pBluescript II (Stratagene) and allowed amplification of Mac-1 cDNA fragments that included the *Not*I site in the linker 5′ to the coding region and the BspEI site at amino acid residue 180 or included the BspEI–BbsI fragment from residue 180 to 672. Mutagenesis of these fragments was done by inverse PCR (24). In brief, a pBluescript II plasmid containing one of the cDNA fragments was amplified by using two mutated primers (GIBCO/BRL), and the linear product was circularized after digestion

The publication costs of this article were defrayed in part by page charge payment. This article must therefore be hereby marked "*advertisement*" in accordance with 18 U.S.C. §1734 solely to indicate this fact.

© 1998 by The National Academy of Sciences 0027-8424/98/954870-6$2.00/0
PNAS is available online at http://www.pnas.org.

Abbreviation: GBP, galactose binding protein; FG-GAP, Phe-Gly, Gly-Ala-Pro.

Data deposition: The atomic coordinates for the Mac-1α β-propeller domain model have been deposited in the Protein Data Bank, Biology Department, Brookhaven National Laboratory, Upton, NY 11973 (reference 1A8X).

*To whom correspondence should be addressed. e-mail: springer@sprsgi.med.harvard.edu.

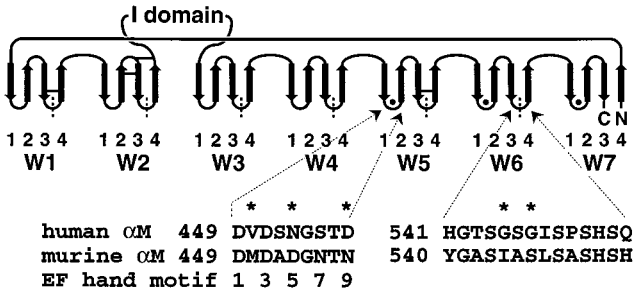

FIG. 1. Topology of the β-propeller model for the N-terminal half of the integrin α-subunit. Each β-sheet (W) contains four anti-parallel β-strands. The Ws are packed into a toroid and around a pseudosymmetry axis in a central cavity that is lined with strand 1 of each W. The FG-GAP repeats, demarcated by vertical dashed lines, are staggered with respect to the Ws. Putative calcium binding loops contain filled circles, and predicted disulfide bonds of Mac-1 are shown by horizontal bars. The I domain is inserted in the loop that connects W2 and W3. The human and mouse Mac-1 amino acid sequences of loop 1–2 of W5 and loop 3–4 of W6 are shown. Residues that contribute to the epitope recognized by mAb CBRM1/20 are indicated with an asterisk. Residues that ligate Ca^{2+} by sidechains (1, 3, 5, 9) or backbone carbonyl O (7) in EF hands are numbered.

with a class 2s restriction enzyme, BsaI. The mutated cDNA fragments were excised from purified plasmid with *Not*I and BspEI or BspEI and BbsI and swapped into the wild-type construct. Human β2 cDNA was excised from CDM8 (25) with *Xba*I and cloned into the *Xba*I site of pCDNA3.1+. PCRs were performed with *Pfu* DNA polymerase (Stratagene), and the constructs were verified by sequence analysis. Plasmid DNA for transfection was prepared by QIAprep Spin Kit or Maxi Kit (Qiagen, Chatsworth, CA).

Tissue Culture, Transfection, and Cell Preparation. COS-7 cells grown in 10-cm tissue culture dishes in RPMI 1640 medium supplemented with 10% fetal bovine serum (JRH Biosciences, Lenexa, KS) and gentamicin (GIBCO/BRL) were cotransfected by using DEAE dextran with 10 μg of α-subunit and 2.5 μg of β-subunit cDNA (26). Transfected cells were replated after treatment with trypsin–EDTA 48 h after transfection and were detached 24 h later with 5 mM EDTA. Approximately 40% expressed Mac-1 as shown by flow cytometry. Human neutrophils were isolated from the whole blood of healthy volunteers by dextran sedimentation, Histopaque 1077 (Sigma) gradient centrifugation at room temperature, and hypotonic lysis at 4°C (27). To vary the divalent cation concentration, the purified neutrophils were washed twice in HE buffer [10 mM Hepes/137 mM NaCl/2.7 mM KCl, pH 7.4/0.2% human serum albumin (Calbiochem)] containing 4 mM EDTA, then twice in HE buffer, and finally twice in HE buffer supplemented as indicated with 2 mM EDTA or EGTA and/or with the indicated concentrations of cations. In immunofluorescent labeling, the same buffer was used for washes and dilution of primary antibodies and fluorescein isothiocyanate goat anti-mouse IgG.

mAb Binding. Mac-1 α-chain-specific mAbs were CBRM1/10, CBRM1/20, CBRM1/29, CBRM1/30, and CBRM1/32 (28) and CBRN1/6 and CBRN3/4 (Na, S. and T.A.S., unpublished data). The myeloma IgG1 control was X63 (American Type Culture Collection). Purified CBRM1/20 IgG was diluted from a 1 mg/ml stock in PBS to 5 μg/ml. Other antibodies were diluted 1 to 200 from ascites. Cells were incubated for 40 min in 96-well plates with each mAb and then, after washing twice, with fluorescein isothiocyanate goat anti-mouse IgG (Zymed) diluted 1 to 50 for 30 min followed by three washes. Neutrophils were washed and incubated in buffers described above, and COS-7 cells were washed and incubated in L-15 medium (Sigma) at 4°C. Cells were fixed in buffer with 1% formaldehyde before flow cytometry for measurement of fluorescence intensity. At least 2,500 cells were acquired on a FACScan instrument (Becton Dickinson).

Molecular Modeling and Sequence Comparison. Modeling was done with SEGMOD (29) of LOOK, version 2.0.5 (Molecular Applications Group, Palo Alto, CA) and MODELLER Release 4 (*http://guitar.rockefeller.edu/modeller*) (30). Templates were 1 tbg, 1 gof, and 2 gbp (*http://www.pdb.bnl.gov*). The packing quality of the models was evaluated with QUACHK of WHAT IF (http://www.sander.embl-heidelberg.de/whatif/) (31).

RESULTS

A Discontinuous Epitope in the β-Propeller Domain. To test the β-propeller model, we searched for a mouse mAb to human Mac-1 (αMβ2) that would recognize an epitope containing residues from different FG-GAP repeats. Initially, 28 different Mac-1α subunit chimeras were constructed. In each chimera, 1 of the 28 predicted loops in the β-propeller model contained murine instead of human sequence. mAbs were tested for reactivity with the α-subunit chimeras coexpressed with the human β-subunit in COS cells. Binding of mAb CBRM1/20 was abolished by two different mutations: hu(W5L1–2)mo, in which the 1–2 loop of W5 was substituted, and hu(W6L3–4)mo, in which the 3–4 loop of W6 was substituted (Table 1). These loops are almost 100 residues apart in the primary structure (Fig. 1). Substitution of the 26 other loops with murine sequence had no effect on mAb CBRM1/20 binding but did allow localization of mAbs CBRM1/32, CBRN1/6, and CBRN3/4 to individual loops in the predicted β-propeller domain (data not shown). The mutations that abrogated CBRM1/20 binding had no effect on binding of these three other β-propeller mAbs, the mAb CBRM1/29 to the I domain (Table 1), or mAbs CBRM1/10 or CBRM1/30 to the C-terminal region (data not shown).

The epitope recognized by mAb CBRM1/20 was localized further with single human-to-mouse amino acid substitutions (Table 1). Three of these substitutions in the 1–2 loop of W5, all in the EF hand-like Ca^{2+}-binding motif, abolished or decreased binding of CBRM1/20 (Table 1). Of these, D457N was expressed on the surface at a level lower than the wild type, as shown with the other mAbs (Table 1). However, binding of mAb CBRM1/20 was decreased much more than binding of other mAbs and therefore appeared to be affected specifically. In the 3–4 loop of W6, the substitution of Gly 547 to Ser abolished binding of mAb CBRM1/20 completely. The substitution Gly 545 to Ile consistently decreased binding to 50% of the wild type.

Model of the Mac-1 β-Propeller Domain. A model of the predicted β-propeller domain of Mac-1 was built by using SEGMOD (29) of LOOK and an alignment (3) with the β-propeller domain of the β-subunit of the G protein transducin (G β) (16). The loops in integrins are longer than in G β (3), and the 3–4 loop in W5 of the galactose oxidase β-propeller domain (17) was used as the template for the longer 3–4 loops of W5–7 in integrins.

The Ca^{2+}-binding motifs in the 1–2 loops of W5–7 in integrins were the most challenging modeling problem. Whereas in the integrin β-propeller model the Ca^{2+}-binding motif occurs in a hairpin turn between β-strands, in the EF hand motif, the Ca^{2+}-binding site occurs in the loop between two α-helices (32). In the EF hand motif, the residues that coordinate Ca^{2+} directly or through a water molecule are in positions 1, 3, 5, 7, 9, and 12 of a 12-residue consensus sequence. A similar sequence motif and structure for residues 1–9 is found in galactose binding protein (GBP); however, the loop is between an α-helix and a β-strand, and the sixth coordination is from a glutamic acid residue that is distal in the sequence but in an adjacent, parallel β-strand. However, the GBP Ca^{2+} binding site as a whole adopts a conformation very similar to the EF hand sites (33). Among different EF hands

Table 1. Binding of mAb to Mac-1 α subunit mutants carrying human-to-mouse substitutions in the 1-2 loop of W5 and the 3-4 loop of W6*

Mutation	CBRM 1/20	CBRM 1/32	CBRN 1/6	CBRN 3/4	CBRM 1/29
	Binding (% of human wild-type ± SD)				
hu(W5L1-2)mo	0 ± 1	103 ± 9	101 ± 11	103 ± 12	104 ± 3
V450M	0 ± 2	87 ± 1	97 ± 2	86 ± 11	103 ± 4
S452A	107 ± 4	99 ± 5	93 ± 10	100 ± 2	91 ± 4
N453D	5 ± 3	101 ± 1	96 ± 2	99 ± 14	106 ± 0
S455N	93 ± 3	113 ± 8	108 ± 5	109 ± 12	107 ± 8
D457N	14 ± 4	70 ± 7	72 ± 11	71 ± 7	61 ± 7
hu(W6L3-4)mo	1 ± 1	104 ± 5	111 ± 6	106 ± 8	111 ± 3
H541Y	96 ± 12	97 ± 2	97 ± 9	106 ± 24	97 ± 4
T543A	104 ± 5	95 ± 2	100 ± 4	94 ± 0	90 ± 15
G545I	51 ± 1	95 ± 5	90 ± 1	95 ± 12	99 ± 5
S546A	92 ± 1	100 ± 1	98 ± 1	98 ± 2	100 ± 7
G547S	0 ± 1	92 ± 0	102 ± 14	84 ± 8	91 ± 1
I548L	108 ± 1	106 ± 7	93 ± 9	105 ± 2	106 ± 0
P550A	122 ± 6	97 ± 4	100 ± 18	83 ± 21	90 ± 16
Q554H	92 ± 1	102 ± 24	104 ± 14	116 ± 11	94 ± 19

*COS-7 cells were cotransfected transiently with cDNAs for the mutated or wild-type Mac-1 α-subunit and human β2-subunit. Cells were stained with mAbs, and fluorescein isothiocyanate anti-IgG in L15 medium, which contains 1.26 mM Ca^{2+} and the % positive cells relative to wild-type, was determined after subtracting staining with X63 myeloma IgG.

and GBP, the structurally most conserved region is residues 1–6 (32). By using this six-residue region as a structural template (Fig. 2) but with no restraints on its orientation relative to the β-propeller domain and by placing 2.4 ± 0.1 Å restraints on the distances between Ca^{2+} and putative oxygen ligands in EF hand motif positions 1, 3, 5, 7, and 9, MODELLER (30) was used to build the 1–2 loops into the LOOK model (Figs. 2 and 3). The average packing quality for the final model was −1.62 as evaluated with QUACHK of WHATIF. For comparison, "a molecule is certain to be incorrect if the score is below −3.0. Poorly refined molecules, very well energy minimized misthreaded molecules and low homology models give values between −2.0 and −3.0. The average quality of 200 highly refined Xray structures was −0.5+/−0.4" (31).

The Spatial Proximity of Residues in the CBRM1/20 Epitope in the β-Propeller Model. The 1–2 and 3–4 loops in β-propellers are the loops that form the lower surface (Fig. 1). In G β and galactose oxidase, the 1–2 loops of each W are in contact with the 3–4 loops of the following W but not the preceding W, thus predicting the contact between the 1–2 loop of W5 and the 3–4 loop of W6, which bear the CBRM1/20 epitope. These loops are longer in integrins than in G β, decreasing prediction accuracy, but indeed are predicted to be in close proximity (Fig. 3). In the model, the three antigenic residues in the 1–2 loop of W5 are 15.8 ± 4.2 Å from the two antigenic residues in the 3–4 loop of W6, based on their Cα atom positions.

Metal Ion Dependence of CBRM1/20 Binding. Cation requirements for binding of mAb CBRM1/20 were investigated by using flow cytometry. CBRM1/20 binding to Mac-1 on purified neutrophils required Ca^{2+}, and Ca^{2+} titration showed that half-maximal binding of mAb CBRM1/20 was obtained at a concentration of 0.2 mM (Fig. 4). Binding of three other mAbs that were mapped to the β-propeller domain was

```
W5              strand 1          strand 2         strand 3       strand 4
strand pos.     01 b2345          6543210          123456         65b4321
G beta      NIICGI.TSVSFSKS.....GRLLLAGYD.......DFNCNVWDal....kaDRAGVLAGH. 311
GO W5       ........................................hiitLGEPGTSPntvf...... 426
Mac-1       QIGAYFGASLCSVdydsngstdLVLIGAPHYYEQTRGGQVSVCPLPRGRARWQCDAVLYGEQ 498
GBP         .............DLNKDG........................................... 139

W6              strand 1          strand 2       strand 3        strand 4
strand pos.     01 b2345          6543210        123456          65b4321
G beta      ...DNRV.SCLGVTDD.....GMAVATGSW.....DSFLKIWN.340 45.mRTRRTLRGH.  54
GO W5       ........................................hiitLGEP.GTSPntvf...... 426
Mac-1       GQPWGRFGAALTVLgdvngdkltDVAIGAPGEEDNRGAVYLFHGTSGSGISPSHSQRIAGSK 560
GBP         ............... DLNKDG........................................ 139
```

FIG. 2. The portion of the structural alignment relevant to W5 and W6 of the Mac-1 β-propeller. The propeller domain of the G protein transducin (16) (G β) and part of the β-propeller of galactose oxidase (17) (GO W5) were used as structural templates for homology modeling with SEGMOD of LOOK. Three 3–4 loop templates of W5 of galactose oxidase were superimposed by using residues shown in lowercase on the transducin G protein β-subunit (17). Superpositions are not shown for W7 but were analogous to those for W5 and W6. The combined template with selected residues shown in uppercase, together with the previous alignment for W1–4 and W7 (3), was used to make a SEGMOD model. The 1–2 loops then were excised from W5–7 of this model, and residues of Mac-1 shown in uppercase together with six residues of the calcium binding loop of GBP (33) for W5, W6, and W7 were used as a template for a further model with MODELLER with Ca^{2+} restraints as described in the text. Residue positions in the sequences are shown, and ladder positions in the β-strands of G β are indicated above the alignment. Antigenic residues of the Mac-1 sequence, as defined by mAb CBRM1/20, are underlined.

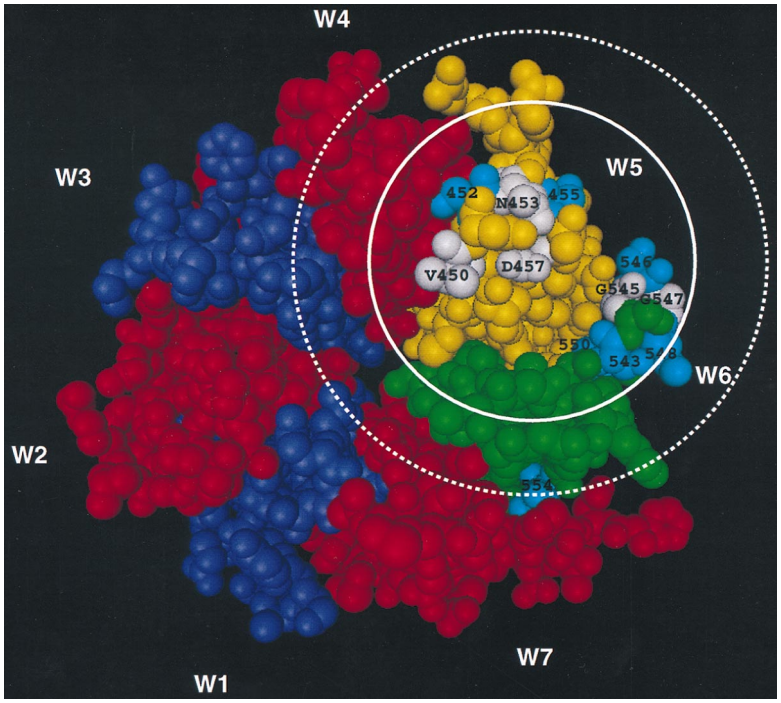

FIG. 3. The β-propeller domain of the Mac-1 α-chain modeled as described in the text and Fig. 2. W1 and W3 are purple, W2, W4, and W7 are red, W5 is yellow, and W6 is green. This view shows the lower face of the β-propeller with residues that, when substituted, decrease binding of mAb CBRM1/20 in white and labeled with residue and number. Residues that, when substituted, did not affect binding are colored turquoise and numbered. Antibodies generally bury a surface area on protein antigens of 700–800 Å^2 (43, 44). A solid circle 700 Å^2 in area shows the approximate size of the mAb CBRM1/20 epitope. Enough free space must be available around the epitope to admit an antibody Fab domain. The dimensions of an antibody's $V_H V_L$ domain are $\approx$32 Å $\times$ 42 Å in the plane of the antigen binding surface. A dotted circle with a diameter of 42 Å is drawn to emphasize this.

identical in the absence and presence of divalent cations (Fig. 4). Sr^{2+} supported CBRM1/20 mAb binding as well as calcium. Ba^{2+} supported binding markedly less well than Ca^{2+} or Sr^{2+}. In 2 mM EDTA, or in 1 mM Mg^{2+} or 1 mM Mn^{2+}, binding was abolished completely (data not shown).

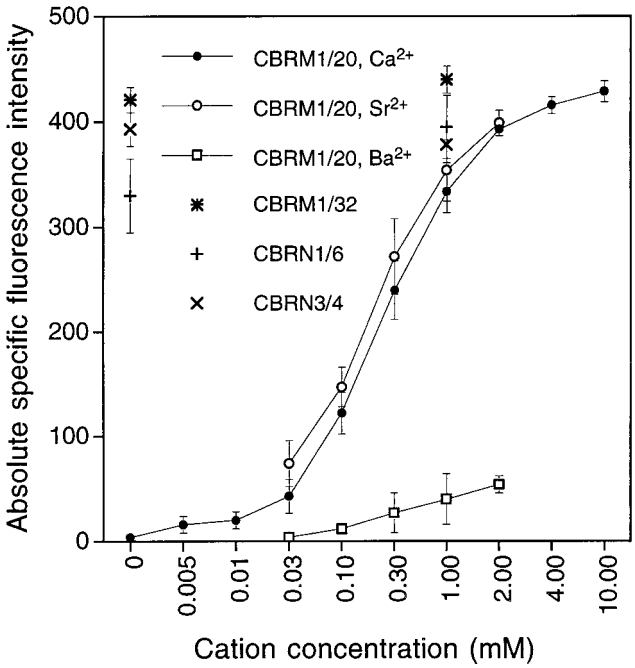

FIG. 4. Divalent cation dependence of mAb CBRM1/20 binding to purified human neutrophil leukocytes. Neutrophils were washed with EDTA, then were washed and stained with mAb CBRM1/20 in the presence of the indicated divalent cation concentrations and were subjected to immunofluorescence flow cytometry. Mean fluorescence intensity is shown with intensity of X63 control staining subtracted. Fluorescence intensity is shown for mAbs CBRM1/32, CBRN1/6, and CBRN3/4 at 0 and 1 mM Ca^{2+}.

The mutants N453D, D457N, and G545I that showed decreased rather than abolished CBRM1/20 binding were incubated with CBRM1/20 in the presence 10 mM Ca^{2+}. Binding of antibody was identical to that in the physiological buffer with 1.26 mM Ca^{2+} used above (data not shown). Hence, the decreased antibody binding of these mutants is not due to a lowered affinity for calcium.

DISCUSSION

We have found that a Ca^{2+}-dependent epitope on integrin Mac-1 recognized by the mAb CBRM1/20 includes residues 94 positions apart in the amino acid sequence of the α-chain. The residues are in different FG-GAP repeats, and if these folded as separate domains, they would be expected to be separated widely. However, the β-propeller model predicts that these residues are present in loops that are adjacent in the three-dimensional structure. They are 15.8 $\pm$ 4.2 Å apart in the model and thus could fit easily within an antibody epitope $\approx$30 Å in diameter. The residues that are most energetically important for protein–protein interactions are in a "hotspot" near the center of the interface (34), and the observed distances would allow both loops to be present in the central region of an epitope. Our results are highly consistent with the predicted β-propeller fold. An alternate model has been proposed for FG-GAP repeats 5 and 6 of the integrin lymphocyte function-associated antigen-1 based on the α-helical EF hand modules of calmodulin (35). In this model, the loops bearing the antigenic residues are on opposite sides of the protein, and the antigenic residues are 37.7 $\pm$ 3.7 Å apart, as determined from a model made with LOOK based on the published alignment (35). Our data, therefore, can rule out this model, which also is not supported by secondary structure or

threading predictions (3). However, the question may be asked whether other folds also could be consistent with the experimental data. To address this question, the probability of finding residues on the surface of proteins within ≤15.8 Å of one another by chance alone was calculated. All proteins in the Protein Data Bank (Upton, NY) that are <30% identical in sequence with one another and have polypeptide chains of >200 residues were used. This database contained 456 chains and was representative of all fold classes. The distance between all residues i and j that are 85 to 105 sequence positions apart and on the protein surface as shown by >20% solvent accessibility or both on the surface and in loops was calculated. The average distance also was calculated from residues i, i + 3, and i + 7 to residues j and j + 2, where j to i ranged from 85 to 105. This relationship mimics that between the five residues in the antigenic determinant for CBRM1/20 mAb. By using these four different distance distributions calculated by A. Sali and A. Badretdinov (Rockefeller University, New York), the probability of finding residues ≤16.5 Å apart by chance alone was found to range from 5.5 to 6.5%. Almost identical distributions were obtained with proteins in which loops are grouped together on opposite ends of the protein, as in the integrin I domain. We conclude that the β-propeller domain fits the experimental data significantly better than random domains, with $P \approx 0.06$.

The evidence that recognition of human Mac-1 by mAb CBRM1/20 depends on Ca^{2+} and is abolished or decreased by three different human-to-mouse substitutions that are within a cation-binding motif in the 1–2 loop of W5 suggests that this mAb acts as a probe of Ca^{2+} binding to this loop. The EC_{50} for Ca^{2+} is 0.2 mM. The K_d for Ca^{2+} may differ if mAb binding alters the affinity of the site for Ca^{2+} but should approximate the observed EC_{50}. The importance of Ca^{2+} in maintenance of α/β-subunit association, in modulating ligand binding, and in regulating exposure of activation epitopes has received wide support (18, 20, 21, 36). In these types of assays, Ca^{2+} is effective in the 0.1–1 mM range, in excellent agreement with our results. Direct measurement of Ca^{2+} binding to low affinity sites in proteins is technically difficult; published measurements of calcium binding to integrins or integrin fragments yield K_d values that vary >1,000-fold, from μM to mM (19, 37–39).

There are important similarities and differences between EF hand and integrin Ca^{2+}-binding motifs (Table 2). The Asp in position 1 is almost invariant in both motifs; its two side chain oxygens set up the turn in the EF hand loop, with one coordinating Ca^{2+} and the other accepting a hydrogen bond from the mainchain NH of the residue in position 6 (32). The Gly in position 6 of the EF hand motif promotes a 90° turn in the chain. It is in a position of the Ramachandran plot common for Gly but not other residues; Gly is less abundant in this position in integrins. The primary structure of the integrin calcium binding site deviates further in several ways. In the integrins, position 5 is always Asp or Asn, in contrast to the EF hands, where other residues also occur. Furthermore, the obligate hydrophobic residues in position 8 of the EF hand are not conserved in the integrins. Except for basic residues, almost any residue is found in this position in integrins and is often charged or polar and is rarely hydrophobic. Finally, the integrin loop has a highly conserved Asp in position 9, in contrast to the EF hand, where several different residues are found (Table 2). The deviations from the EF hand motif, especially in positions 5, 6, 8, and 9, suggest a variant mode of coordination. In particular, the constraints on a turn between adjacent β-strands make it likely that the position of the residue in position 9 differs, correlating with the preference for Asp in integrins but not in EF hands. Our model suggests that this residue in integrins may have a coordination position more similar to that of the Glu in position 12 of EF hands. As to the one "missing" coordination position in integrins, we can find no conserved, acidic residue distant in sequence but close in the model structure, analogous to that in GBP. The K_d for calcium measured here is higher than in EF hands and GBP (10^{-5} to 10^{-9} M), possibly reflecting the lack of a 12th coordination position. EF hands and GBP prefer Ca^{2+} over Sr^{2+} by $\approx 10^3$ and Ca^{2+} over Ba^{2+} by $>10^5$ (40), indicating a constraining force acting against expansion of the cavity to accommodate the increasing ionic radii of Sr^{2+} and Ba^{2+}. The lack of preference between Ca^{2+} and Sr^{2+} of the integrin Ca^{2+} binding site as probed by mAb CBRM1/20 suggests that the protein ligands do not encapsulate completely the ion (40), which again is consistent with at least one coordination site being exposed to solvent.

The loss of antigenicity after the N453D and D457N mutations is most interesting because these residues occupy positions 5 and 9 in the Ca^{2+} binding motif and their sidechain oxygen atoms are predicted to ligate Ca^{2+}. Their backbone, not sidechain atoms, are predicted to be exposed to antibody. We predict that the change between acidic and amide sidechain alters ligation or hydrogen bonding around the Ca^{2+}, resulting in a change in backbone conformation that is detected by the antibody. It is striking that, of 117 integrin calcium binding motifs surveyed (Table 2), W5 of murine Mac-1 is the only one with an Asn in position 9. The Asp in position 5 of that loop may compensate for the lack of the acidic residue in position 9. The consistently poorer expression seen after mutation of

Table 2. Residues in positions 1 through 9 of the integrin calcium binding site present in FG-GAP repeat 4 of some and repeats 5, 6, and 7 of all integrins compared with the corresponding residues in EF hand calcium binding sites

Residue or residue group	Sequence Position								
	1	2	3	4	5	6	7	8	9
	% abundance in integrins, % abundance in EF hands								
D	97, 99	0, 0	41, 76	3, 2	79, 47	5, 1	0, 1	8, 0	96, 34
N	0, 0	0, 1	48, 22	9, 8	21, 24	1, 2	2, 1	13, 0	1, 4
E	3, 0	0, 7	1, 0	4, 2	0, 1	0, 0	3, 7	9, 0	3, 13
Q	0, 0	0, 11	0, 0	18, 5	0, 0	0, 1	1, 4	9, 0	0, 2
ST	0, 0	0, 16	9, 1	5, 3	0, 29	14, 0	8, 30	23, 0	0, 34
G	0, 0	0, 0	1, 0	34, 53	0, 0	68, 93	0, 0	1, 0	0, 12
AVLICM	0, 0	91, 26	0, 1	12, 1	0, 0	2, 1	30, 12	15, 100	0, 1
P	0, 0	0, 0	0, 0	0, 0	0, 0	0, 0	0, 0	23, 0	0, 0
FYW	0, 0	9, 2	0, 0	0, 0	0, 0	1, 0	54, 27	0, 0	0, 0
HRK	0, 0	0, 36	0, 0	15, 26	0, 0	9, 2	3, 19	1,0	0, 0

Residues in the calcium binding sites (a total of 117) from all available integrin sequences were counted. The EF hand sequences were taken from ref. 45. Only eucaryotic EF hand sequences with observed or inferred calcium binding that had no insertion or deletion (a total of 498 calcium binding sequences) were analyzed. The residues are given by one-letter code.

the Asp453 to Asn but not after mutation of Asn457 to Asp suggests that at least one of the two residues in positions 5 and 9 may have to be an Asp for proper expression.

We have localized the mAb CBRM1/32 to the 2–3 loop of W6 and the mAbs CBRN1/6 and CBRN3/4 to the 3–4 loop of W4 of Mac-1 (Lu, C., C.O., and T.A.S., unpublished data). Binding of these antibodies is unaffected by removal of Ca^{2+}. Therefore, conformational changes induced by removal of calcium are limited to specific regions of the β-propeller domain. It has been proposed widely that the Ca^{2+} binding motifs of integrins play a direct role in ligand binding by integrins. Our localization of the CBRM1/20 binding site to the Ca^{2+} binding motif in W5 rules out a direct role for this site in ligand binding by Mac-1 because mAb CBRM1/20 does not inhibit binding to four different ligands (6). The β-propeller model suggested that the upper rather than lower face of this domain is involved in ligand recognition (3). This view received further support from analysis of the interaction between the non-I domain containing integrin $\alpha 4\beta 1$ and vascular cell adhesion molecule 1 (41).

The area on the lower surface of the β-propeller domain bound by mAb CBRM1/20 (Fig. 3) cannot be occupied at the same time by other integrin domains or subunits, creating important implications for whether the central cavity in the β-propeller is filled. All seven- and eight-bladed β-propellers except G β have a central cavity along the pseudosymmetry axis that is filled with a prosthetic group or, in the case of galactose oxidase, with a polypeptide finger extending from another domain (3, 16, 17). The central cavity in G β, which appears to be the closest structural homologue of the integrin β-propeller, contains only solvent. Strand 1 and the 1–2 loop of W5 form one side of this channel. Although the domain from which the polypeptide finger extends into the central cavity in galactose oxidase contains only 100 residues, it binds to all seven 1–2 loops as shown by burial of solvent-accessible surface on at least 2 and an average of 3.1 residues in each loop. An analogous domain in integrins would make a 1–2 loop less accessible in an antibody epitope. We therefore believe that it is more likely that the central cavity will be free, as it is in G β. In the absence of a coordinating residue in the polypeptide finger, it would be unlikely that a divalent cation could be ligated in the central cavity, as might have been conceived by analogy to galactose oxidase (3). Thus, our data on mAb epitopes not only supports the β-propeller domain hypothesis but also is beginning to provide hints, by a process of elimination, of where interfaces with other domains may lie. It appears that the β-propeller domain in the integrin α-subunit has important interactions with the integrin β-subunit because mAbs that bind to four different epitopes on the Mac-1 β-propeller domain, including CBRM1/20, do not react in the absence of the β-subunit (Lu, C., C.O., and T.A.S., unpublished data). Similar results have been obtained with lymphocyte function-associated antigen-1 (42). Our results interpreted in light of the β-propeller model make it unlikely that the Ca^{2+} in the 1–2 loop of W5 could ligate the β-subunit and suggest that an indirect role for Ca^{2+} in stabilizing association between the α- and β-subunits should be given serious consideration.

We thank Andrej Sali, Azat Badretdinov, and Roberto Sánchez for help with MODELLER. We thank Martin Hemler and Michael N. G. James for refereeing the manuscript. C.O. was supported by a fellowship from The Danish Natural Science Research Council. This work was supported by National Institutes of Health Grant CA31799.

1. Springer, T. A. (1990) *Nature (London)* **346,** 425–433.
2. Hynes, R. O. (1992) *Cell* **69,** 11–25.
3. Springer, T. A. (1997) *Proc. Natl. Acad. Sci. USA* **94,** 65–72.
4. Tuckwell, D. S., Brass, A. & Humphries, M. J. (1992) *Biochem. J.* **285,** 325–331.
5. Loftus, J. C., Smith, J. W. & Ginsberg, M. H. (1994) *J. Biol. Chem.* **269,** 25235–25238.
6. Diamond, M. S., Garcia–Aguilar, J., Bickford, J. K., Corbi, A. L. & Springer, T. A. (1993) *J. Cell Biol.* **120,** 1031–1043.
7. Michishita, M., Videm, V. & Arnaout, M. A. (1993) *Cell* **72,** 857–867.
8. Huang, C. & Springer, T. A. (1995) *J. Biol. Chem.* **270,** 19008–19016.
9. Springer, T. A. (1994) *Cell* **76,** 301–314.
10. Diamond, M. S. & Springer, T. A. (1994) *Curr. Biol.* **4,** 506–517.
11. Ginsberg, M. H. (1995) *Biochem. Soc. Trans.* **23,** 439–446.
12. Loftus, J. C. & Liddington, R. C. (1997) *J. Clin. Invest.* **99,** 2302–2306.
13. Lee, J.-O., Rieu, P., Arnaout, M. A. & Liddington, R. (1995) *Cell* **80,** 631–638.
14. Qu, A. & Leahy, D. J. (1995) *Proc. Natl. Acad. Sci. USA* **92,** 10277–10281.
15. Murzin, A. G. (1992) *Proteins* **14,** 191–201.
16. Sondek, J., Bohm, A., Lambright, D. G., Hamm, H. E. & Sigler, P. B. (1996) *Nature (London)* **379,** 369–374.
17. Ito, N., Phillips, S. E. V., Stevens, C., Ogel, Z. B., McPherson, M. J., Keen, J. N., Yadav, K. D. S. & Knowles, P. F. (1991) *Nature (London)* **350,** 87–90.
18. Jennings, L. K. & Phillips, D. R. (1982) *J. Biol. Chem.* **257,** 10458–10466.
19. Rivas, G. A. & Gonzalez–Rodriguez, J. (1991) *Biochem. J.* **276,** 35–40.
20. Hu, D. D., Barbas, C. F., III & Smith, J. W. (1996) *J. Biol. Chem.* **271,** 21745–21751.
21. Dransfield, I., Cabañas, C., Craig, A. & Hogg, N. (1992) *J. Cell Biol.* **116,** 219–226.
22. Hemler, M. E. (1990) *Annu. Rev. Immunol.* **8,** 365–400.
23. Corbi, A. L., Kishimoto, T. K., Miller, L. J. & Springer, T. A. (1988) *J. Biol. Chem.* **263,** 12403–12411.
24. Stemmer, W. P. C. & Morris, S. K. (1992) *BioTechniques* **13,** 215–220.
25. Hibbs, M. L., Wardlaw, A. J., Stacker, S. A., Anderson, D. C., Lee, A., Roberts, T. M. & Springer, T. A. (1990) *J. Clin. Invest.* **85,** 674–681.
26. Aruffo, A. & Seed, B. (1987) *Proc. Natl. Acad. Sci. USA* **84,** 8573–8577.
27. English, D. & Anderson, B. R. (1974) *J. Immunol. Methods* **5,** 249–252.
28. Diamond, M. S. & Springer, T. A. (1993) *J. Cell Biol.* **120,** 545–556.
29. Levitt, M. (1992) *J. Mol. Biol.* **226,** 507–533.
30. Sali, A. & Blundell, T. L. (1993) *J. Mol. Biol.* **234,** 779–815.
31. Vriend, G. (1990) *J. Mol. Graph.* **8,** 52–56.
32. Strynadka, N. C. J. & James, M. N. G. (1989) *Annu. Rev. Biochem.* **58,** 951–998.
33. Vyas, N. K., Vyas, M. N. & Quiocho, F. A. (1987) *Nature (London)* **327,** 635–638.
34. Wells, J. A. (1996) *Proc. Natl. Acad. Sci. USA* **93,** 1–6.
35. Stanley, P., Bates, P. A., Harvey, J., Bennett, R. I. & Hogg, N. (1994) *EMBO J.* **13,** 1790–1798.
36. Bazzoni, G., Shih, D.-T., Buck, C. A. & Hemler, M. A. (1995) *J. Biol. Chem.* **270,** 25570–25577.
37. D'Souza, S. E., Ginsberg, M. H., Matsueda, G. R. & Plow, E. F. (1991) *Nature (London)* **350,** 66–68.
38. Steiner, B., Cousot, D., Trzeciak, A., Gillessen, D. & Hadvary, P. (1989) *J. Biol. Chem.* **264,** 13102–13108.
39. Gulino, D., Boudignon, C., Zhang, L., Concord, E., Rabiet, M.-J. & Marguerie, G. (1992) *J. Biol. Chem.* **267,** 1001–1007.
40. Falke, J. J., Drake, S. K., Hazard, A. L. & Peersen, O. B. (1994) *Q. Rev. Biophys.* **27,** 219–290.
41. Irie, A., Kamata, T. & Takada, Y. (1997) *Proc. Natl. Acad. Sci. USA* **94,** 7198–7203.
42. Huang, C. & Springer, T. A. (1997) *Proc. Natl. Acad. Sci. USA* **94,** 3162–3167.
43. Davies, D. R., Padlan, E. A. & Sheriff, S. (1990) *Annu. Rev. Biochem.* **59,** 439–473.
44. Davies, D. R. & Cohen, G. H. (1996) *Proc. Natl. Acad. Sci. USA* **93,** 7–12.
45. Kawasaki, H. & Kretsinger, R. H. (1994) *Protein Profile* **1,** 343–517.